Journal of Nuclear Materials 405 (2010) 50–58

Contents lists available at ScienceDirect

Journal of Nuclear Materials

journal homepage: www.elsevier.com/locate/jnucmat

An XPS study on the evolution of type 304 stainless steel surface during routine TCSU operation

A. Tankut *, K.E. Miller, G.C. Vlases

University of Washington, Redmond Plasma Physics Laboratory, Redmond, WA 98052, USA

ARTICLE INFO

Article history:
Received 9 September 2009
Accepted 23 July 2010

ABSTRACT

A surface analysis study was carried out to monitor the first-wall evolution in the Translation, Confinement, and Sustainment Upgrade (TCSU) experiment. A type 304 stainless steel sample was exposed to processes including the standard ex-situ surface preparation, helium glow discharge cleaning (He-GDC), plasma discharges, and backfilling the vacuum chamber with filtered N_2. After each process, the sample was carried to a surface analysis chamber for X-ray photoelectron spectroscopy (XPS), using a custom designed in-vacuum transfer device. Results indicated that He-GDC was effective in removing both physically and chemically bound carbon and oxygen on the stainless steel surfaces due to the physical impact of the glow. The plasma discharges resulted in oxidation on the surface. The use of filtered nitrogen during vacuum breaks was verified as an effective method for minimizing carbon and oxygen contamination.

Published by Elsevier B.V.

1. Introduction

The original Translation, Confinement, and Sustainment (TCS) experiment was devised to study rotating magnetic field (RMF) assisted field reversed configuration (FRC) plasmas in the Redmond Plasma Physics Laboratory of University of Washington, and operated for about 3 years between 2002 and 2004 [1,2]. The TCS experiment was categorized within the smaller scaled fusion research experiments alternative to the tokamaks, known as Innovative Confinement Concepts (ICCs) [3]. The studies in TCS demonstrated that it was possible to form and sustain FRCs using RMF alone, without the need of a high-voltage short pulse initiator. The plasmas produced in TCS were the first FRCs to be such as field reversed theta pinches. The plasmas produced in TCS were the first FRCs to be sustained. Since the plasma lifetime was many times longer than a particle lifetime, τ_p, plasma–wall interaction became important for the first time in FRC research. However, the TCS plasmas suffered from low temperatures limited to around 30 eV. Two possible causes were identified for the limited temperatures: impurity radiation and the innate effect of RMF on the closed field lines of FRCs [2]. To acquire a true assessment of the premise of RMF assisted FRCs, therefore, the minimization of impurity radiation was imperative. The TCS Upgrade (TCSU) experiment was built with the objective of minimizing impurity radiation. Accordingly, extensive effort was given to the ex-situ preparation of plasma-facing (vacuum-facing) surfaces during construction, as well as in situ wall-conditioning capabilities such as glow discharge cleaning (GDC) and plasma-assisted chemical vapor deposition (PACVD) techniques [4]. Furthermore, a surface science oriented study of the plasma–wall interactions was undertaken to understand impurity formation and its ingestion into the plasma.

The interaction processes that occur between the plasma edge and the surrounding wall surfaces are quite complex and vary in nature and extent. The wall surface chemistry is critical to plasma performance, as it can influence processes including desorption, trapping, and sputtering [5]. While most of the processes that directly affect the plasma occur within several monolayers of the surface, the impact of the plasma on the wall could extend much deeper and may have long term consequences [6]. The wall surface history becomes especially important for research experiments where different wall conditioning techniques are frequently tested and utilized. Although surface analysis tools have been extensively utilized in mainstream tokamak research experiments, the study of plasma–wall interactions using a surface analytical approach has not been widespread among the ICCs. The present study aims to be an example of materials science oriented research for the ICC community. The choice of stainless steel (SS) as the studied material also has relevance in this context; while most Tokamak research has moved to advanced plasma-facing materials (e.g.,

* Corresponding author. Address: Redmond Plasma Physics Lab, Univ. of Washington, 14700 NE 95th St., #100, Redmond, WA 98052, USA. Tel.: +1 425 881 7706; fax: +1 425 882 9137.
E-mail address: aydin@u.washington.edu (A. Tankut).

0022-3115/$ - see front matter Published by Elsevier B.V.
doi:10.1016/j.jnucmat.2010.07.035

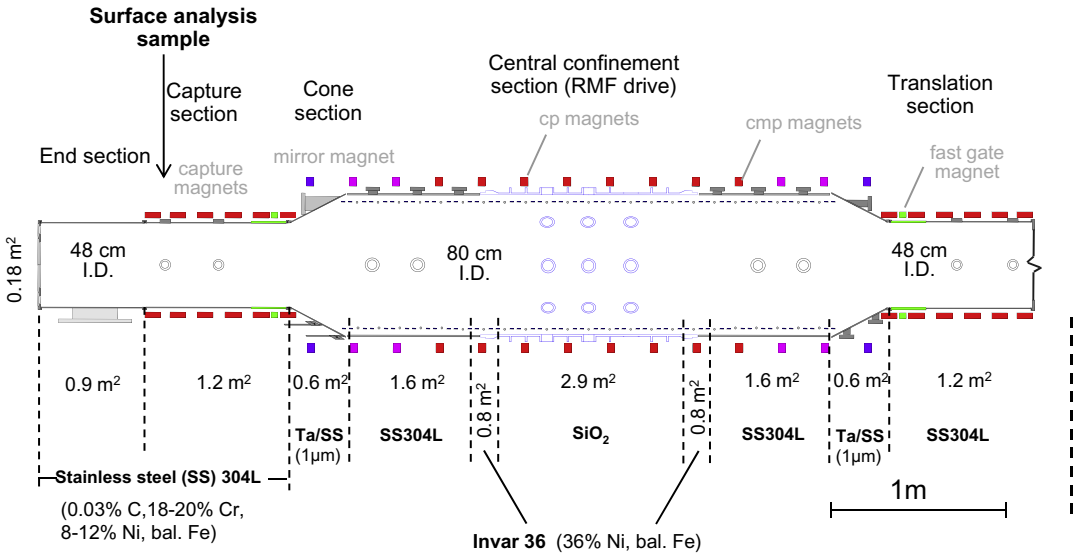

Fig. 1. Scale schematic of TCSU main chamber showing various sections and first wall materials with corresponding surface area.

graphite, W, Be), SS still constitutes majority of the first wall of ICCs.

2. Materials and methods

2.1. First wall materials in TCSU

A scaled schematic of the TCSU confinement section is given in Fig. 1, with various first wall materials labeled. The confinement section consists mainly of stainless steel type 304. A quartz chamber was located at the center to enable RMF penetration. The plasma is formed and sustained inside the quartz chamber. The cone sections, initially type 304, were coated with a Ta layer of a nominal thickness of 1 μm. Finally, in order to relieve potential stresses, bellows made from an iron–nickel alloy, Invar 36, were placed between the stainless and quartz chambers.

To study the evolution of wall surfaces during routine operation of TCSU, a series of studies was carried out on a sample that was inserted at the location of the wall. A type 304 stainless steel sample, chosen as a representative wall material, was exposed to some of the key processes that were actively employed during the first 2 years of TCSU operation, in the order given below:

- Standard TCSU ex-situ surface preparation.
- Helium glow discharge cleaning.
- TCSU plasma discharges.
- Going up to atmospheric pressures using filtered N_2.

After each process, the sample was transported under high vacuum to the analysis chamber for X-ray photoelectron spectroscopy (XPS).

2.2. Experimental details of the processes

Prior to its insertion into TCSU, the sample was prepared according to the standard stainless steel vacuum surface preparation protocol. The procedure was established for the various stainless steel surfaces of TCSU by comparing samples prepared by different methods using scanning electron microscopy (SEM) and energy dispersive X-ray spectroscopy (EDS). Methods studied included acid etching, ultrasonic cleaning in alcohol, and ultrasonic cleaning in alkali-based soap/detergent solutions. Results suggested that a protocol based on ultrasonic cleaning with an industrial cleaning solution, Micro 90, would be the most practically suitable approach. The surface analysis sample was prepared according to this standard protocol following a mechanical polishing treatment using SiC sandpapers (up to 1000 grit). Details of the procedure are listed in Table 1.

After the 'standard cleaning', the sample was inserted into TCSU and exposed to helium glow discharge cleaning (He-GDC). Details of the TCSU He-GDC can be found in Ref. [4]. The glow was operated at a pressure around 1 Pa, and a mass flow rate around 10^{-3} Pa m^3/s. The electrode voltage was 400 V, with an average current flowing to the wall of 0.1 A/m^2. The sample was exposed to 64 h of glow, corresponding to He ion fluence around 1×10^{24} m^{-2}.

Following the He-GDC process, the sample was exposed to 156 deuterium plasma discharges in TCSU. Typical plasmas during this period were characterized by densities of about 10^{19} m^{-3}, total temperatures ($T_e + T_i$) of 100 eV, and peak fields of 20 mT. The plasma duration was 2.5 ms and the particle confinement time of the FRCs was approximately 0.2 ms. The average deuterium ion fluence to the wall based on these figures would be approximately 2×10^{21} m^{-2}. However, it should be noted that the ion fluence was not uniform throughout the first wall. A direct diagnostic of the ion fluence at the sample was not available at the time of the study.

Finally, the sample was exposed to filtered nitrogen gas as the entire TCSU vacuum system was brought up to atmospheric pressure. The nitrogen gas was run through an SAES FT400-902 filter

Table 1
Ex-situ preparation of stainless steel sample surfaces for exposure to ultra high vacuum (UHV) in TCSU, 'standard cleaning'. The sample surfaces were polished with SiC sand paper prior to cleaning.

1	Initial soap wash and rinse
2	Ultrasonic cleaning in 2% Micro 90 solution in de-ionized (DI) water for 60 min
3	DI water rinse
4	Ultrasonic cleaning in DI water for 30–60 min (repeat steps 3 and 4 as needed)
5	Methanol rinse
6	Drying with compressed N_2

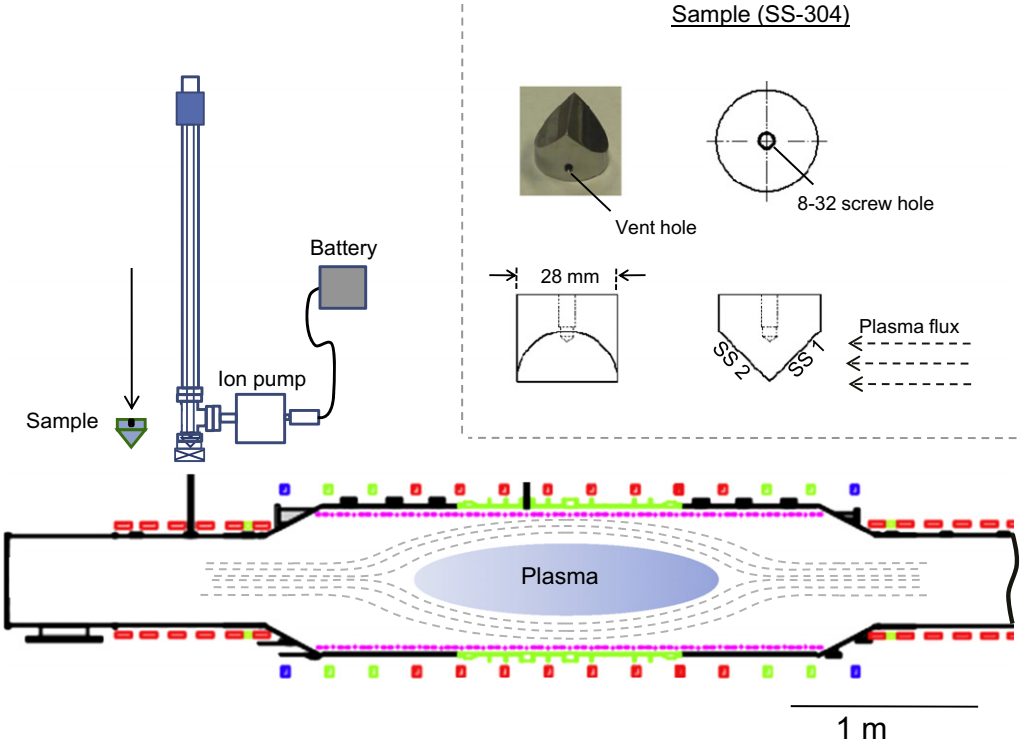

Fig. 2. Sketch of TCSU showing the location of the surface analysis sample (the sample transfer device and the sample are enlarged to show detail). Inset shows a photograph and different views of the sample, as well as the orientation of the sample surface with respect to the plasma flux.

prior to its introduction into TCSU. The filter reduced the concentration of impurities such as H_2O, O_2, CO, CO_2, H_2, to below one part per billion levels. The sample was exposed to the nitrogen back-fill for 30 min, at which point the system was pumped back down. During this process, a slight positive pressure of nitrogen was maintained, and two 3–3/8″ conflat flanges were replaced. The nitrogen flow rate into the chamber during this period was estimated to be 3×10^{-4} m^3/s.

2.3. Sample insertion, withdrawal, and transfer

A sketch of TCSU showing the location for sample insertion is shown in Fig. 2. The sample was inserted using a custom designed in-vacuum sample transfer device that was equipped with a battery operated 2 l/s ion pump. This device maintained pressures at the low 10^{-6} Pa level during sample transfer. The inset in the upper left corner of Fig. 2 shows a close-up sketch of the sample. The sample was made from a stainless steel type 304 cylindrical piece of 28 mm diameter that was faceted 45° off the main axis to create two primary faces, SS1 and SS2. The sample was oriented in TCSU such that SS1 faced the magnetic field lines with incoming plasma, while SS2 was shadowed from plasma by SS1. Thus SS1 was exposed to a significantly higher plasma flux than SS2.

A sketch showing various stages of operation of the sample transfer device is shown in Fig. 3. Initially, the sample transfer device was connected to TCSU through a dedicated port with gate valves on both systems closed (Fig. 3a). The volume separating the transfer device and TCSU was then pumped, and the sample was inserted into TCSU (Fig. 3b). The sample was located to be in line with the surrounding chamber walls. After the sample was exposed to the desired process, it was retracted back to its initial position within the sample transfer device and transferred to the analysis chamber (Fig. 3c). XPS analysis was carried out in the analysis chamber using an Al Kα X-ray source and a double-pass cylindrical mirror analyzer.

3. Results and discussion

3.1. Surface condition after standard cleaning

The condition of the sample surface after standard cleaning is shown by the XPS survey scan in Fig. 4. Despite the removal of the bulk contamination, there was still considerable amount of carbon and oxygen on the surface, together amounting to about 85% of the total XPS signal collected from the surface. The relative peak intensities of Fe, Cr and Ni suggests a Cr rich and Ni depleted surface layer, as would be expected from the passivation metal oxide layer of a type 300 stainless steel [7].

Fig. 5 shows high resolution scans taken from the sample after standard cleaning. Fig. 5a indicates that carbon on the surface consisted mainly of C–C type bonds associated with the surface adventitious carbon, with a peak binding energy at around 285 eV. There was a small, high binding energy shoulder at around 287.6 eV, which could be associated with C–OH (286.7 eV) and/or C–N bonds (287.9 eV) [8]. It is likely that this shoulder was due to C–OH bonding, since the XPS survey scan given in Fig. 4 indicates no nitrogen on the surface. The O_{1s} spectrum in Fig. 5b can be de-convoluted into two major peaks, one caused by surface contamination (~531.8 eV), and one due to the oxygen bound to metals in the stainless steel passivation layer (~529.8 eV). Fe and Cr are predominantly in their oxide states, as shown in Fig. 5c and d, respectively. Ni seems to be mostly metallic (Fig. 5e), which was expected due to its relatively stable metallic state.

3.2. Surface condition after 64 h He-glow discharge cleaning

A comparison of the XPS survey scans taken from sample surface SS1 before and after 64 h of He-GDC is shown in Fig. 6. He-GDC resulted in a near-complete removal of carbon and a significant reduction of oxygen content on the sample surface. The physically adsorbed layer is held on the surface by weak Van der Waals

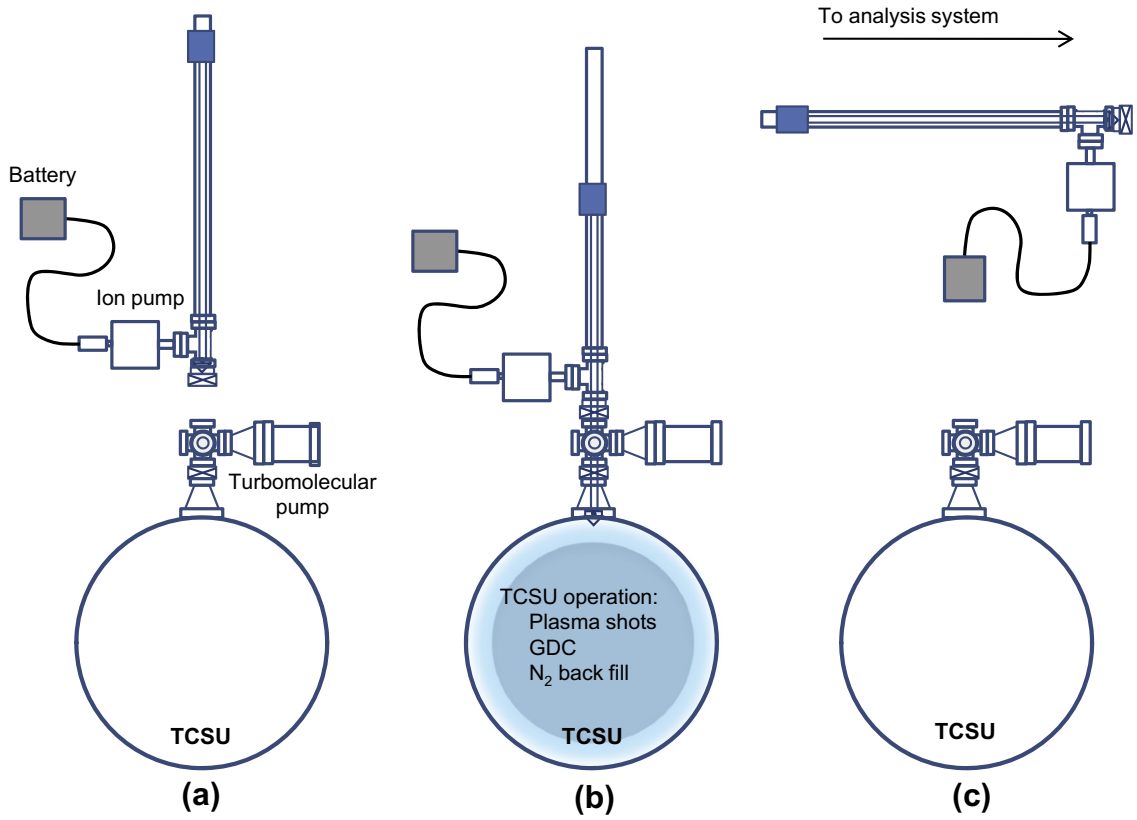

Fig. 3. Sample insertion into TCSU and transfer to analysis chamber: (a) sample insertion into TCSU, (b) exposure of sample to TCSU operation and (c) sample transfer to analysis system.

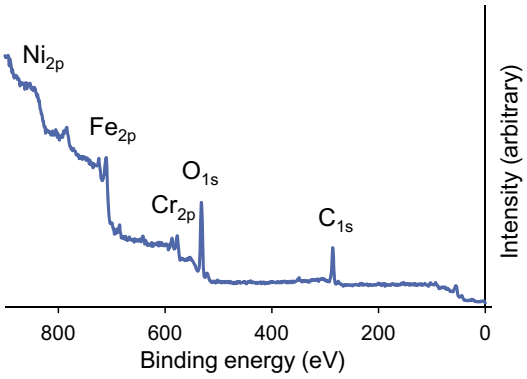

Fig. 4. XPS survey scan taken from the sample surface following the TCSU standard cleaning protocol.

forces, with typical bond energies on the order of a few tenths of an eV. It can therefore be assumed that the glow discharge ions, with impact energies of 100s of eV, removed the surface carbon by particle-induced desorption.

The removal of the physically adsorbed contamination layer was confirmed by comparing the high resolution O_{1s} spectra taken before and after 64 h of He-GDC, as shown in Fig. 7. The high energy peak associated with the C–O and H–O was reduced considerably, and remaining oxygen on the surface was mainly bound to metal oxides in the passivation layer.

The high resolution XPS spectra taken from the sample surface before and after 64 h of He-GDC are shown for Fe_{2p3} in Fig. 8a and b, respectively, and for Cr_{2p3} in Fig. 8c and d, respectively. For both species, significant increase in metallic states was observed after He-GDC. Moreover, the Fe–OH peak disappeared in the Fe_{2p3} spectrum upon exposure to glow. The chemical reduction of metal oxides by the glow discharge ions, as described previously for hydrogen GDC [7,9], cannot be valid in the case of chemically inert helium. Accordingly, two alternative mechanisms can be suggested for the emergence of metallic Fe and Cr on the stainless steel surface after He-GDC.

The first mechanism involves the chemical reduction of the MO layer by residual hydrogenic species. A residual gas analysis (RGA) scan taken from TCSU prior to He-GDC is shown in Fig. 9. It can be seen that the TCSU vacuum was dominated by three peaks at 2, 3, and 4 a.m.u. These correspond to H_2, DH and D_2 and/or He, respectively. It is well known that type 300 stainless steels contain large amounts of hydrogen [10], while deuterium was trapped in the chamber walls during plasma discharges. It can therefore be speculated that these residual hydrogenic species might have played a role in the reduction of the metal oxides, by reacting with the free oxygen/carbon bonds created by the He-glow discharge.

Studying the removal of oxygen and carbon in stainless steel during He-GDC, Wang et al. have proposed the following series of reactions [11]:

$$\mathrm{He} + \mathrm{Wall} \rightarrow \mathrm{H} + \mathrm{C} \quad (1)$$

$$2\mathrm{H} + \mathrm{MO} \rightarrow \mathrm{H_2O} + \mathrm{M} \quad (2)$$

$$\mathrm{H_2O} + \mathrm{C} \rightarrow \mathrm{CO} + \mathrm{H_2} \quad (3)$$

Eq. (2) is equivalent to the hydrolysis of metal oxides in the case of H-GDC on stainless steel, which has been proposed to occur in two steps [7]:

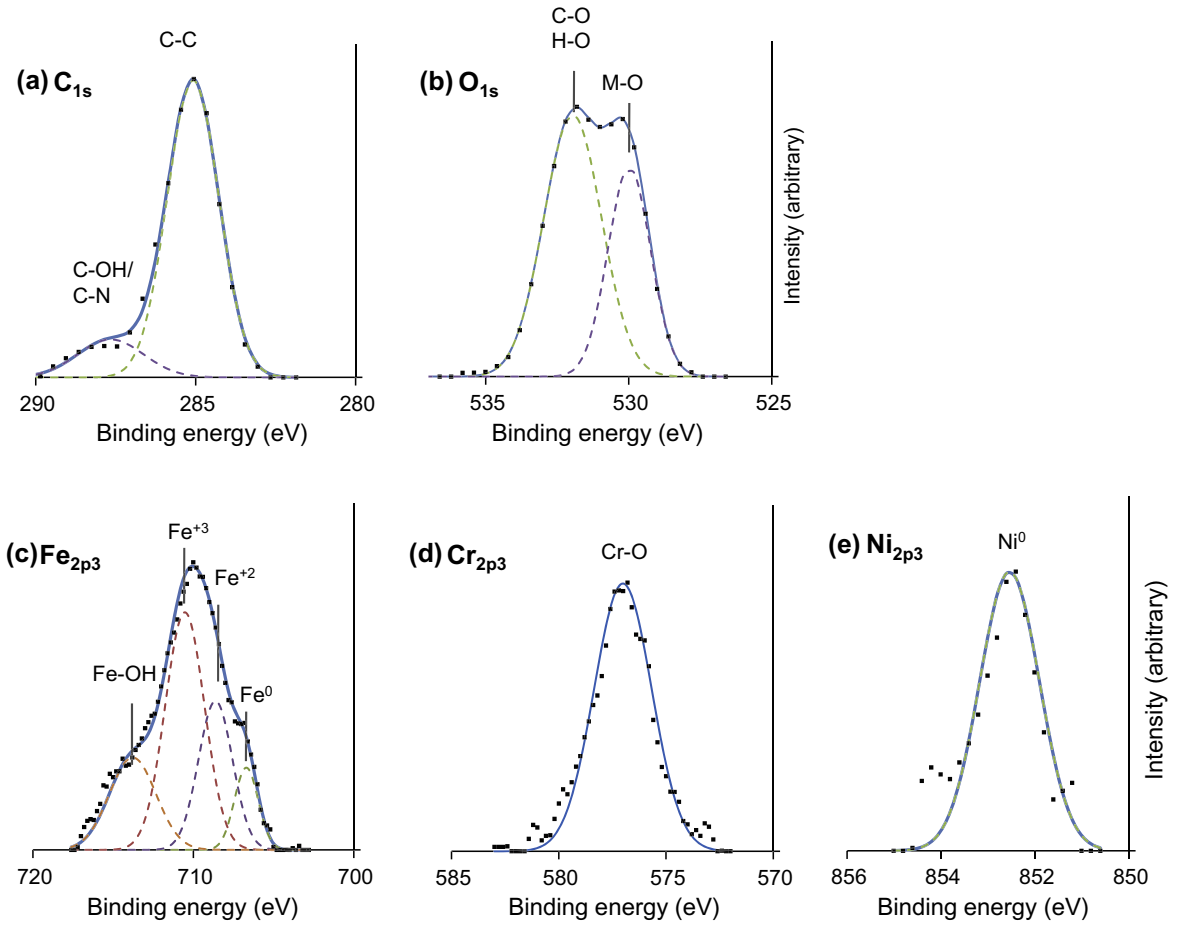

Fig. 5. High resolution XPS spectra taken from sample surface prepared with TCSU standard cleaning protocol: (a) C_{1s}, (b) O_{1s}, (c) Fe_{2p3}, (d) Cr_{2p3}, and (e) Ni_{2p3}.

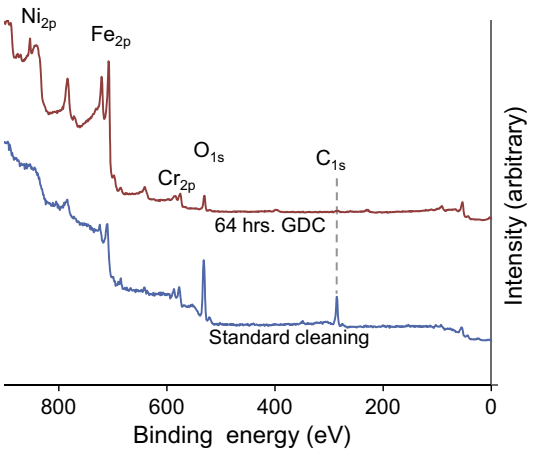

Fig. 6. Comparison of survey scans taken before and after He-GDC on the sample surface. The two spectra are placed on the same graph for ease of comparison; their absolute values on the vertical axis are irrelevant.

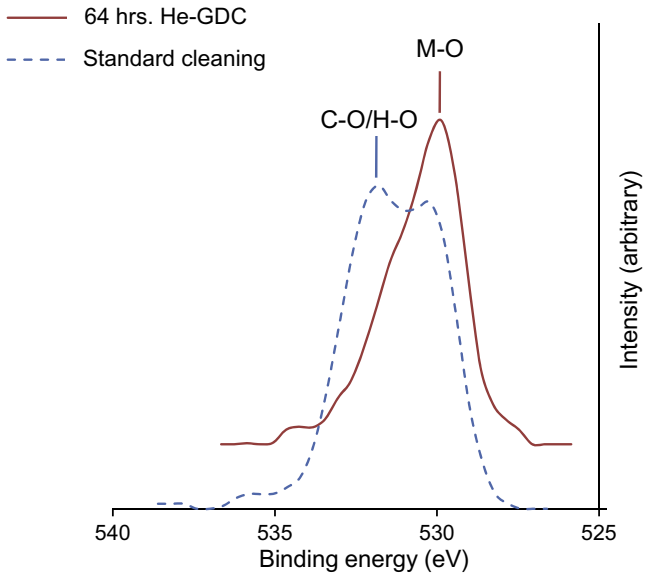

Fig. 7. Comparison of high resolution O_{1s} spectra taken from SS1 before and after He-GDC. The two spectra are placed on the same graph for ease of comparison; their absolute values on the vertical axis are irrelevant.

$$MO + H \rightarrow MOH \quad (4)$$

$$MOH + H \rightarrow M + H_2O \quad (5)$$

However, this mechanism is inadequate in explaining our observations from the sample analysis. First, it has been previously documented that H-GDC effectively reduces Fe and Ni oxides while Cr oxides, which are chemically much more stable, remain unaffected [7,12]. In our system, the Cr_{2p3} XPS scans show a significant reduction in Cr oxides, with no detectable metallic Cr present prior to the He-GDC (Fig. 8c), and considerable metallic Cr following the

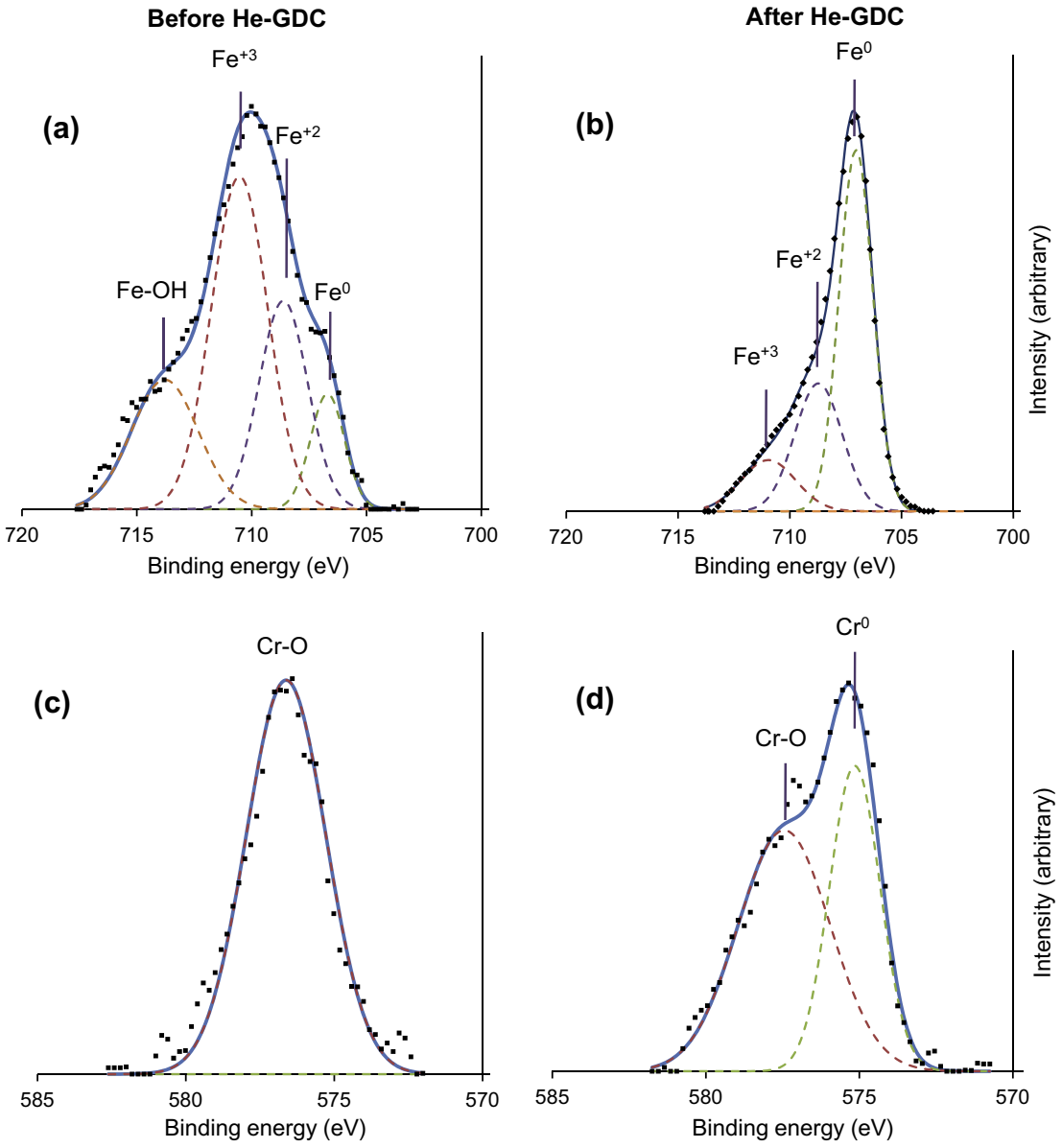

Fig. 8. High resolution XPS Fe_{2p3} and Cr_{2p3} spectra taken from SS1 before and after He-GDC: (a) Fe_{2p3} before He-GDC, (b) Fe_{2p3} after He-GDC, (c) Cr_{2p3} before He-GDC, and (d) Cr_{2p3} after He-GDC.

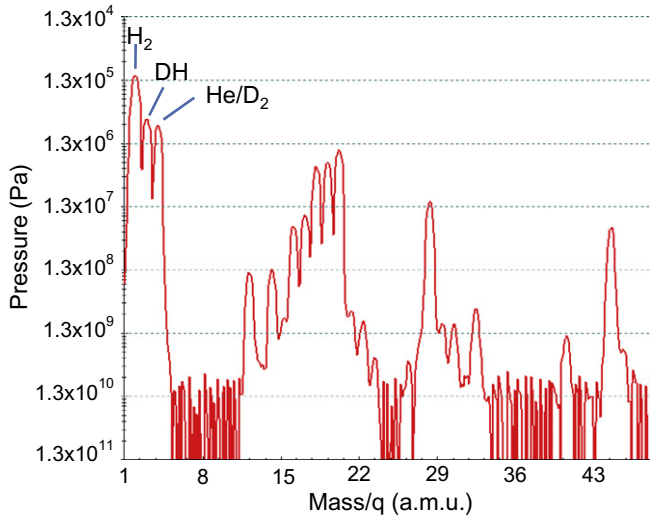

Fig. 9. RGA scan taken from TCSU prior to He-GDC.

glow (Fig. 8d). Second, H-GDC results in the formation of $Fe(OH)_x$ on the surface, as a result of the first step of the hydrolysis reaction, Eq. (4) [7,9]. On the contrary, the high resolution Fe_{2p3} XPS scan taken after He-GDC (Fig. 8b) indicates no Fe–OH peak formation. Rather, the Fe–OH peak that made up to about 20% of the Fe_{2p3} signal prior to He-GDC (Fig. 8a) was reduced sufficiently to become undetectable after the glow.

The second mechanism that could explain the observed reduction of Fe and Cr oxides involves sputtering and/or diffusion of metal oxides due to the physical impact of He-GDC. During the glow discharge process, ions are accelerated towards the walls (cathode) and strike the wall surface at energies close to the plasma potential. This potential was about 400 eV for TCSU He-GDC. At such energies, the ion impact can alter the physical structure of the surface.

In TCSU, He-GDC sputtered the stainless steel chamber walls, and re-deposited the stainless steel components on neighboring first-wall surfaces. This effect was readily observed at the macroscopic level, as transparent surfaces became opaque from the redeposition of sputtered material. Fig. 10 shows an SEM micrograph

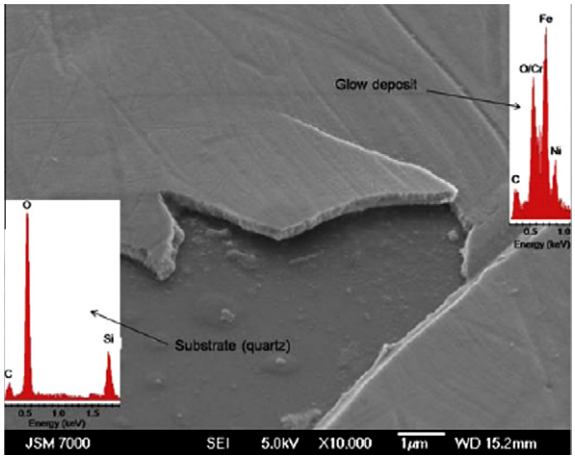

Fig. 10. Scanning electron micrograph of a quartz view port, surface exposed to extensive He-GDC (~300 h) in TCSU, with corresponding EDS spectra.

taken from a quartz viewing port that was exposed to extensive He-GDC (~300 h), along with the EDS scans taken from the coating and the bare substrate. The spectroscopical analysis of the deposited film showed that the deposited film consisted mainly of Fe, Cr, and Ni. While a quantitative characterization of the sputtering during He-GDC has not been performed, it would not be unreasonable to suspect that a considerable amount of the stainless steel passivation layer of the sample migrated elsewhere during 64 h of He-GDC, leading to a decrease in the passivation layer thickness. Thus, metallic species from the bulk metal layer were incorporated in the XPS scans.

The collision cascades instigated by the energetic He ions could also have played role in the increase of metallic species on the surface due to diffusion and impact-induced dissociation. A recent study on stainless steel carried out by Tokitani et. al. suggests that considerable damage on the surface was found after 60 h of He-GDC, where the effect of the glow was estimated to reach up to 40 nm into the surface [13]. In such a case, the impact of the glow could cause diffusion in the vicinity of the passivation layer-bulk metal interface, such that the metallic species from the bulk metal could migrate into the near-surface region. Moreover, the ion impact could result in the partial fracture of the M–O bonds, where the split off oxygen is then relocated to interstitial lattice sites [14].

We thus conclude that while a chemical reduction processes might have occurred simultaneously, a combination of mechanisms prompted by the physical impact of the He ions seems to

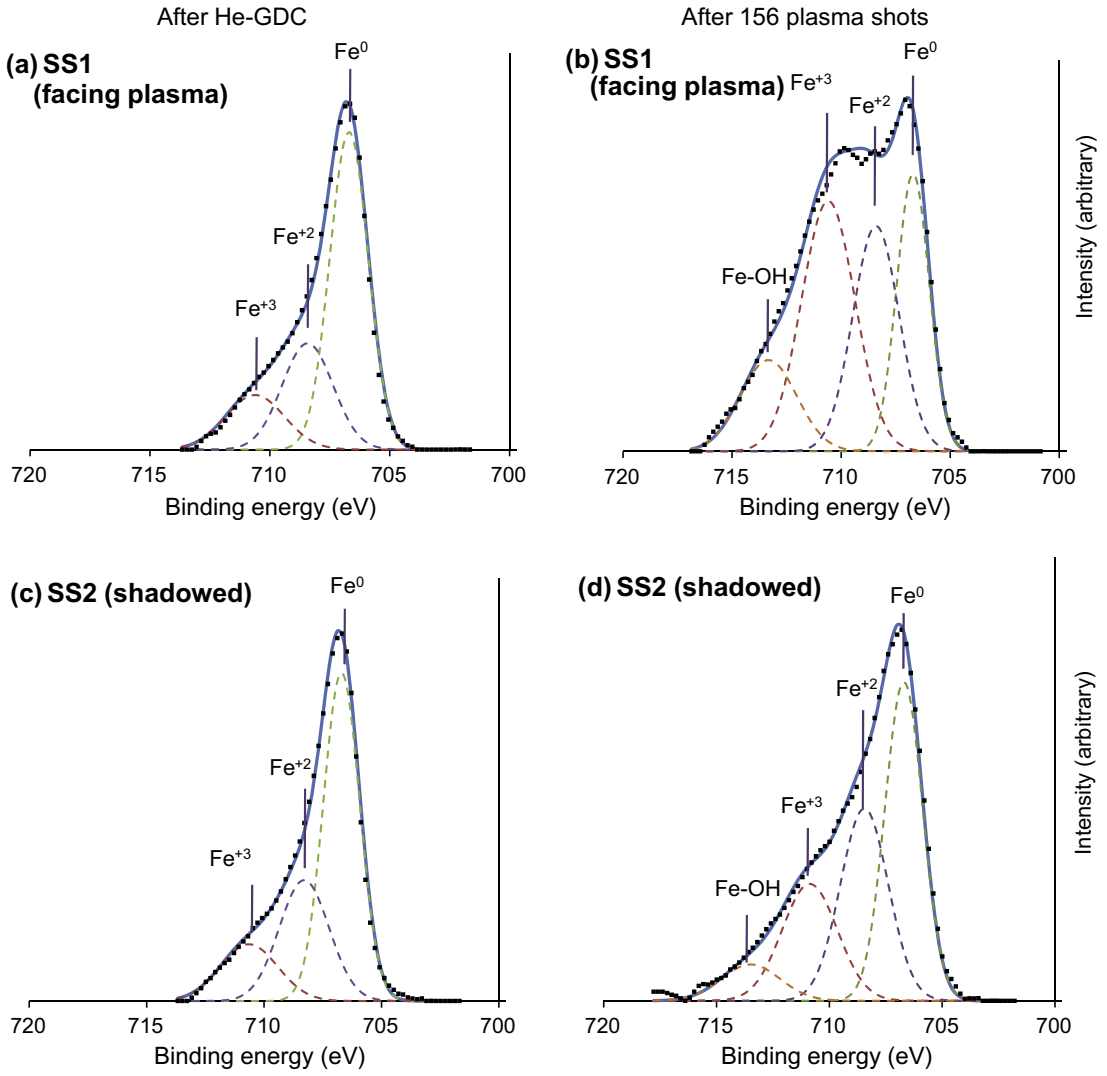

Fig. 11. High resolution XPS Fe_{2p3} spectra taken from SS1 and SS2 before and after 156 plasma shots: (a) SS1 before plasma shots, (b) SS1 after plasma shots, (c) SS2 before plasma shots, and (d) SS2 after plasma shots.

be the more plausible explanation for the increase in the metallic Fe and Cr, as it addresses both the emergence of elemental Cr and the disappearance of $Fe(OH)_x$ after He-GDC.

3.3. Surface condition after exposure to plasma discharges

The high resolution Fe_{2p3} spectra taken from the sample surfaces SS1 and SS2 before and after 156 plasma shots are presented in Fig. 11a–d. When compared to the scan taken from SS1 before the plasma shots (Fig. 11a), an increase in the oxide states can be seen in the Fe_{2p3} spectrum upon exposure to TCSU plasma (Fig. 11b). Moreover, a high energy peak associated with Fe–OH bonding appeared. An increase in oxide states can also be seen on the sample surface facing away from the plasma (SS2) by comparing Fig. 11c and d. However, the effect is considerably smaller, verifying that the plasma flux was the major contributor for the oxidation of the surface.

The oxidation upon exposure to plasma discharges of metallic surfaces is a commonly observed phenomenon [9,15]. While the processes leading to oxidation are not fully understood, the widely accepted explanation involves the dissociation of water released from the surface by plasma impact [16]. The reverse hydrolysis process described earlier for H-GDC (Eqs. (4) and (5)) is applicable to hydrogenic plasmas as well. Energetic hydrogen ions interact with metal oxides near the surface, leading to the formation of water, and its subsequent release. However, the plasma temperature is typically much higher than that of H-GDC, so the released water is rapidly dissociated, ionized, and re-deposited onto the chamber walls. When performing H-GDC, plasma condition and gas flow rates are selected such that the released water is effectively pumped away with minimal ionization and re-deposition. The appearance of $Fe(OH)_x$ observed after plasma shots (Fig. 11b and d) could be due to the first step of the hydrolysis reaction (Eq. (4)) and/or the dissociation of water into H and OH by the plasma.

It is well known that exposure of a fresh metallic surface to atmospheric air results in oxidation of the surface, along with a layer of hydrocarbon and water contamination. To minimize such exposure during TCSU vacuum breaks, purified nitrogen gas was used to bring the system up to atmospheric pressures, as described in Section 2. To assess the effectiveness of this procedure XPS analyses on the sample was performed following a 30 min vacuum break.

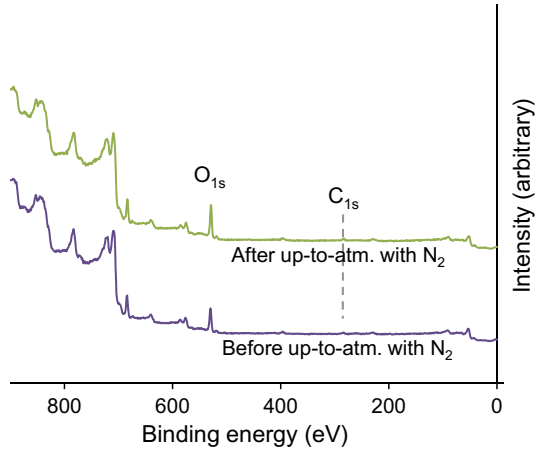

Fig. 12. Comparison of survey scans taken from the sample surface before and after going up to atmospheric pressures with filtered N_2. The two spectra are placed on the same graph for ease of comparison; their absolute values on the vertical axis are irrelevant.

The XPS survey scan from the surface following the vacuum break is shown in Fig. 12. There was no observable increase in the C_{1s} peak, while there was a slight increase in the O_{1s} peak. Comparing the high resolution Fe_{2p3} spectra before (Fig. 13a) and after (Fig. 13b) suggests an increase in the Fe oxide states, particularly for Fe^{+3} and Fe–OH peaks. Though not shown, a similar increase in oxide peak intensity was observed in the Cr_{2p3} spectrum.

Rough calculations to estimate the amount of oxygen introduced into the system during the nitrogen backfill were carried out. Sources considered include impurities in the nitrogen backfill gas, outgassing of two conflat flanges that were replaced during the backfill, and air diffusion into the chamber as the flanges were replaced. None of these sources seem to explain the observed oxidation, as they amount to no more than 1% of a monolayer of oxygen on the wall surface. Other possible mechanisms could include small leaks that might have been present in the nitrogen fill system at the time of the study as well as an anomaly in the SAES filter. At any rate, the amount of oxidation caused by the process was estimated to be equivalent to only about 50 plasma shots (i.e., one typical day of operation). This finding justifies the use of purified

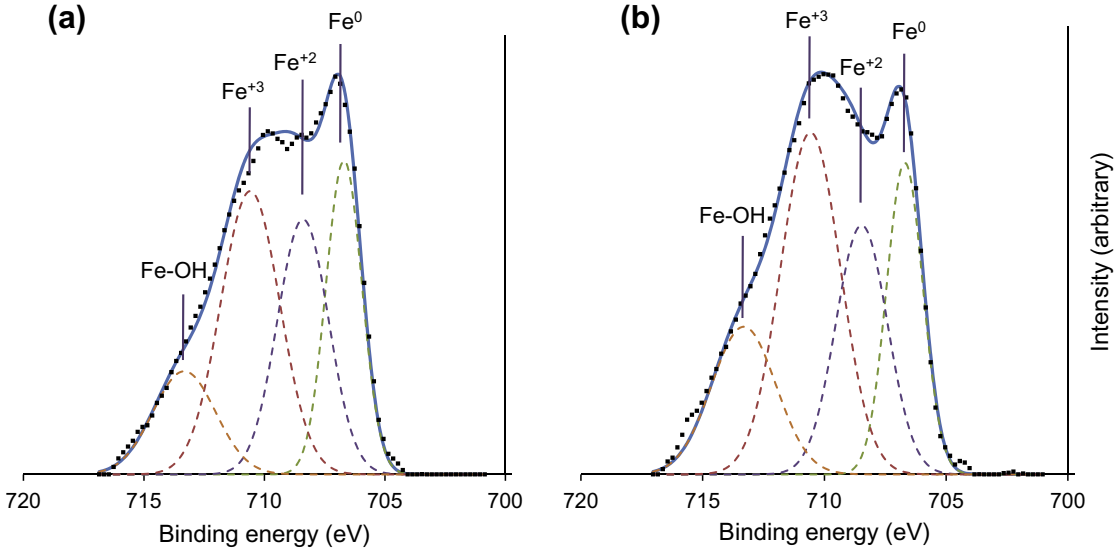

Fig. 13. High resolution XPS Fe_{2p3} spectra taken from sample surface before and after up to atmosphere with N_2 for 30 min: (a) Fe_{2p3} before N_2 and (b) Fe_{2p3} after N_2.

nitrogen during system backfill as a means to minimize air contamination in TCSU. More importantly, it suggests that the system can be brought up to atmospheric pressures as needed, with little fear of contamination.

4. Summary

The effects of different processes employed in TCSU on the stainless steel walls were studied by utilizing a dedicated surface analysis system. A stainless steel 304 sample was inserted into TCSU during each process of concern, and transferred to the analysis chamber subsequently for X-ray photoelectron spectroscopy. The experiments revealed that:

- The standard surface cleaning protocol did not remove all the carbon and oxygen on the stainless surface. Carbon was mainly associated with the adventitious contamination layer, while oxygen was present in both the contamination layer and the metal oxide passivation layer.
- Sixty-four hours of He-GDC resulted in a near-complete removal of the surface contamination layer. Carbon was almost completely removed, and oxygen left on the surface was predominantly bound to metals. The amount of metallic Fe and Cr on the surface increased significantly, probably due to the erosion of the metal oxide layer and/or the diffusion of bulk metallic species towards the surface, both caused by the energetic impact of the glow ions.
- Plasma shots in TCSU resulted in wall oxidation, particularly on the sample surface facing the plasma flux. The oxidation was due to the dissociation of water formed and released from the surface as a product of the reverse hydrolysis reaction, driven by the introduction of hydrogenic species during plasma shots.
- Using filtered N_2 to go up to atmospheric pressures was an effective way to minimize air contamination in TCSU during vacuum breaks. No surface carbon was detected after 30 min of exposure, and the amount of oxidation was comparable to 50 plasma shots.

References

[1] A.L. Hoffman, H.Y. Guo, J.T. Slough, S.J. Tobin, L.S. Schrank, W.A. Reass, G.A. Wurden, Fusion Sci. Technol. 41 (2002) 92.
[2] G.C. Vlases, TCS Edge Studies, Grant DE-FG03-01ER-546537, Final Technical Report, 2005.
[3] S. Woodruff, J. Fusion Energy 26 (2007) 247.
[4] K.E. Miller, J.A. Grossnickle, R.D. Brooks, C.L. Deards, T.E. DeHart, M.E. Dellinger, M.B. Fishburn, B. Hansen, J.W. Hayward, A.L. Hoffman, W.S. Kimball, K.Y. Lee, D.E. Lotz, P.A. Melnik, R.D. Milroy, Z.A. Pietrzyk, G.C. Vlasses, F.S. Ohuchi, A. Tankut, Fusion Sci. Technol. 54 (2008) 946.
[5] P. Staib, H.F. Dylla, S.M. Rossnagel, J. Nucl. Mater. 93–94 (1980) 315.
[6] V. Philipps, P. Wienhold, A. Kirschner, M. Rubel, Vacuum 67 (2002) 399.
[7] H.F. Dylla, J. Nucl. Mater. 93 and 94 (1980) 61.
[8] M. Vinnichenko, Th. Chevolleau, M.T. Pham, L. Poperenko, M.F. Maitz, Appl. Surf. Sci. 201 (2002) 41.
[9] P. Staib, H.F. Dylla, S.M. Rossnagel, J. Vac. Sci. Technol. 17 (1980) 291.
[10] R. Calder, G. Lewin, Brit. J. Appl. Phys. 18 (1967) 1459.
[11] Z. Wang, D. Yan, E. Wang, Plasma Sci. Technol. 4 (2002) 1565.
[12] J. Winter, Plasma Phys. Control. Fusion 38 (1996) 1503.
[13] M. Tokitani, M. Miyamoto, K. Tokunaga, T. Fujiwara, N. Yoshida, A. Komori, S. Masuzaki, N. Ashikawa, S. Inagaki, T. Kobuchi, A. Komori, M. Goto, J. Miyazawa, K. Nishimura, N. Noda, B.J. Peterson, A. Sagara, Nucl. Fusion 45 (2005) 1544.
[14] R. Holm, S. Strop, Appl. Phys. 12 (1977) 1001.
[15] J. Winter, J. Nucl. Mater. 161 (1989) 265.
[16] F. Waelbroeck, J. Winter, P. Wienhold, J. Vac. Sci. Technol. A 2 (1984) 1521.